All-angle behavior in two-body scattering and phenomenological hard strings

Fumihiko Nakamura
Department of Physics, Hiroshima University, Hiroshima 730, Japan
(Received 19 November 1979)

All-angle behavior of the cross sections in two-body scattering is examined by a counting law on the basis of the string structure in a hadron. Then the fixed-angle scaling is interpreted as the contribution of strings at large momentum transfer. This counting law contains a good crossing relation, and predicts the energy dependence and the angular distribution of the cross sections in various processes. In charge-exchange processes the applicability of this model to all-angle cross sections is examined. This model gives a good explanation of the large ratio $[d\sigma(pp)/dt]/[d\sigma(\bar{p}p)/dt]$, the asymmetric distribution of $d\sigma(K^-p\to\pi^+\Sigma^-)/dt$, and the transition behavior between the fixed-angle scaling and the Regge-pole-like behavior.

I. INTRODUCTION

Large-momentum-transfer phenomenology seems to have suggested a probe of the basic dynamics between quarks.[1,2] A fixed-angle scaling is the prominent feature in two-body scattering as well as a power-law scaling of the inclusive production cross section at large momentum transfer. In recent experiments we can see the transition behavior from the fixed-angle scaling to the Regge-pole-like behavior at all angles in various processes.[3-6] There have been attempts to explain large-momentum-transfer phenomena by means of quark counting such as in Refs. 7–11, but they are not always successful even in exclusive reactions. None of them can explain both the large experimental value of $[d\sigma(pp)/dt]/[d\sigma(\bar{p}p)/dt]$ and the asymmetric distribution of $d\sigma(K^-p\to\pi^+\Sigma^-)/dt$.

The feature of the transition from the Regge-pole behavior to fixed-angle scaling seems to be continuous in the experimental cross sections as $-t$ increases. On the other hand, both the Regge trajectory and the dual amplitude are interpreted as the dynamics of a stringlike object.[12,13] Therefore, we try to interpret the fixed-angle scaling as the effect of strings at large momentum transfer.

In previous papers[14] a counting law was proposed on the basis of the number of hard strings in the configuration of quarks and strings, where it was assumed that a hard string has q^{-2} (q = momentum transfer) dependence at large momentum transfer in each channel in the invariant amplitude. This q^{-2} dependence of quark-quark scattering can explain $P_T{}^{-8}$ dependence of meson or jet production cross sections at $2\lesssim P_T\lesssim 8$ GeV, which is consistent with the model by Field and Feynman.[15] The energy and angular dependence of nondiffractive amplitudes is predicted in all the processes of two-body scattering by the above counting law. Consequently, the phenomenological investigation on all-angle cross sections in various processes makes us find the hadron structure with quarks and strings. In general the following types have been considered for a baryon by the string picture[13]: (a) linear type, q-q-q, (b) junction type,

(c) Δ type,

(d) diquark type, q-qq (q denotes a quark; dash denotes a string). The type (a) has two strings, and the types (b) and (c) have three strings. Since in (b) and (c) we need more strings than in (a) to construct a baryon, their contribution is dampened more than that of (a) at large momentum transfer, even if these types are mixed, as long as a hard string has q^{-2} decreasing effect. Here we treat the configuration of (d) as an exception because the diquark state without a string forbids Z-type processes (see Fig. 2), therefore the linear type of (a) has the leading effect. In this paper the applicability of the predictions of the hard-string counting law to all-angle scattering behavior is investigated. Then we analyze recent data of all-angle cross sections in $pn\to pn$, $p^{\pm}p\to p^{\pm}p$, $K^-p\to\bar{K}^0n$ or $\pi^{\pm}\Sigma^{\mp}$, and $\gamma p\to\pi^+n$, and examine the transition behavior between the Regge-pole-like behavior and the fixed-angle scaling one.

The quark bound states by the strings in linear-type configurations are shown in Fig. 1. *It is assumed that only the quark at the end of the string can interact actively in hadron-hadron reactions.* Then the basic states are

$$\text{baryon } q\text{-}q\text{-}q, \quad \text{meson } q\text{-}\bar{q}. \tag{1.1}$$

The excited states are constructed beside the

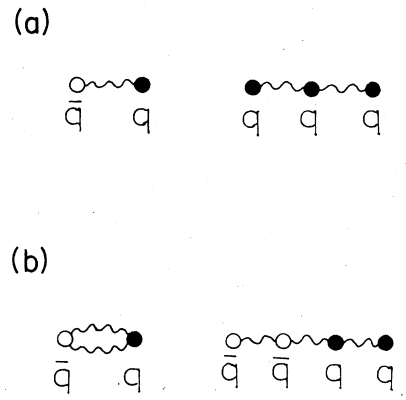

FIG. 1. The allowed states of quarks, (a) the basic states, (b) the excited state.

above configuration by the reaction of q-q-q and $\bar{q}$-$\bar{q}$-$\bar{q}$:

$$q\text{-}q\text{-}\bar{q}\text{-}\bar{q}\,,\quad q\supset\bar{q}\,. \tag{1.2}$$

As shown in Table I, by the above string picture, we can consider various possibilities in the structure of (anti)baryon-baryon scattering amplitude particularly.

In Sec. II the counting law based on the hard string is discussed in detail. In Sec. III the experimental results are compared with our predictions at all angles. In Sec. IV general problems of large-momentum-transfer phenomenology are discussed and a summary is given.

II. A COUNTING LAW ON THE BASIS OF HARD STRINGS

The hadrons are composed of quarks and strings in various configurations as shown in Fig. 1. In hadron-hadron scattering, the various type amplitudes are considered for planar quark-string diagrams in Fig. 2, and the other type diagrams are obtained by s-u or s-t crossing. Here the string is the binding agent between quarks, and should have a quark or an antiquark at its end. The bound states of quarks in reaction have such configurations as q-$\bar{q}$, $q\supset\bar{q}$, q-q-q, $\bar{q}$-$\bar{q}$-$\bar{q}$, and q-q-$\bar{q}$-$\bar{q}$. In two-body hard scattering all the strings have large momentum transfer in each channel, where it is demanded that the quarks have finite momentum fraction of the parent hadron. So, at large momentum transfer, a string gives a uniform dynamical effect, q^{-2} dependence, to the amplitude.

TABLE I. The predictions of our hard-string counting law (in parentheses) are compared with the results of experiments. For two-body scattering, $T\sim\tilde{s}^{-n_s}\tilde{t}^{-n_t}\tilde{u}^{-n_u}$,

$$\frac{d\sigma}{dt}\sim f(\theta)s^{-N},$$

$$R(a/b)=\frac{(d\sigma/dt)(a)}{(d\sigma/dt)(b)}\bigg|_{\theta=90^\circ}$$

where $N=2(n_s+n_t+n_u)+2$ ($x\leftrightarrow y$: x-y crossing) at $s\to\infty$.

	n_s	n_t	n_u	N	Experiment (our predictions)
Meson-meson					
H	1	1	0	6	
$X\,[H(s\leftrightarrow u)]$	0	1	1		
$Z\,[H(t\leftrightarrow u)]$	1	0	1		
Meson-baryon					
H	1	2	0	8	In $\pi^{\pm}p$ and $K^{\pm}p$,
$X\,[H(s\leftrightarrow u)]$	0	2	1		$N=7.5$–8.5
Z	2	0	2	10	$(N=8)$
$H_t\,[H(s\leftrightarrow t)]$	2	1	0	8	$(N=10$ for $K^-p\to\pi^+\Sigma^-)$
$X_t\,[X(s\leftrightarrow t)]$	2	0	1		$R(K^+p/K^-p)=3.0$–2.0
$Z_t\,[Z(s\leftrightarrow t)]$	0	2	2	10	$(R(X/H)=4)$
(Anti)baryon-baryon					
H	1	3	0	10	In pp
H_c	2	2	0		$N=9.5$–11.5
$H_d\,[H(s\leftrightarrow t)]$	3	1	0		
$X\,[H(s\leftrightarrow u)]$	0	3	1		$R(pp/\bar{p}\bar{p})\sim 100$
$X_c\,[H_c(s\leftrightarrow u)]$	0	2	2		$(R(pp/\bar{p}\bar{p})=64)$
$X_d\,[H_d(s\leftrightarrow u)]$	0	1	3		$(R(\Sigma^-p/\bar{\Sigma}^+p)=4)$
					$(R(np\to\Delta^-\Delta^{++}/\bar{\Delta}^+p\to\bar{n}\Delta^{++})=4)$

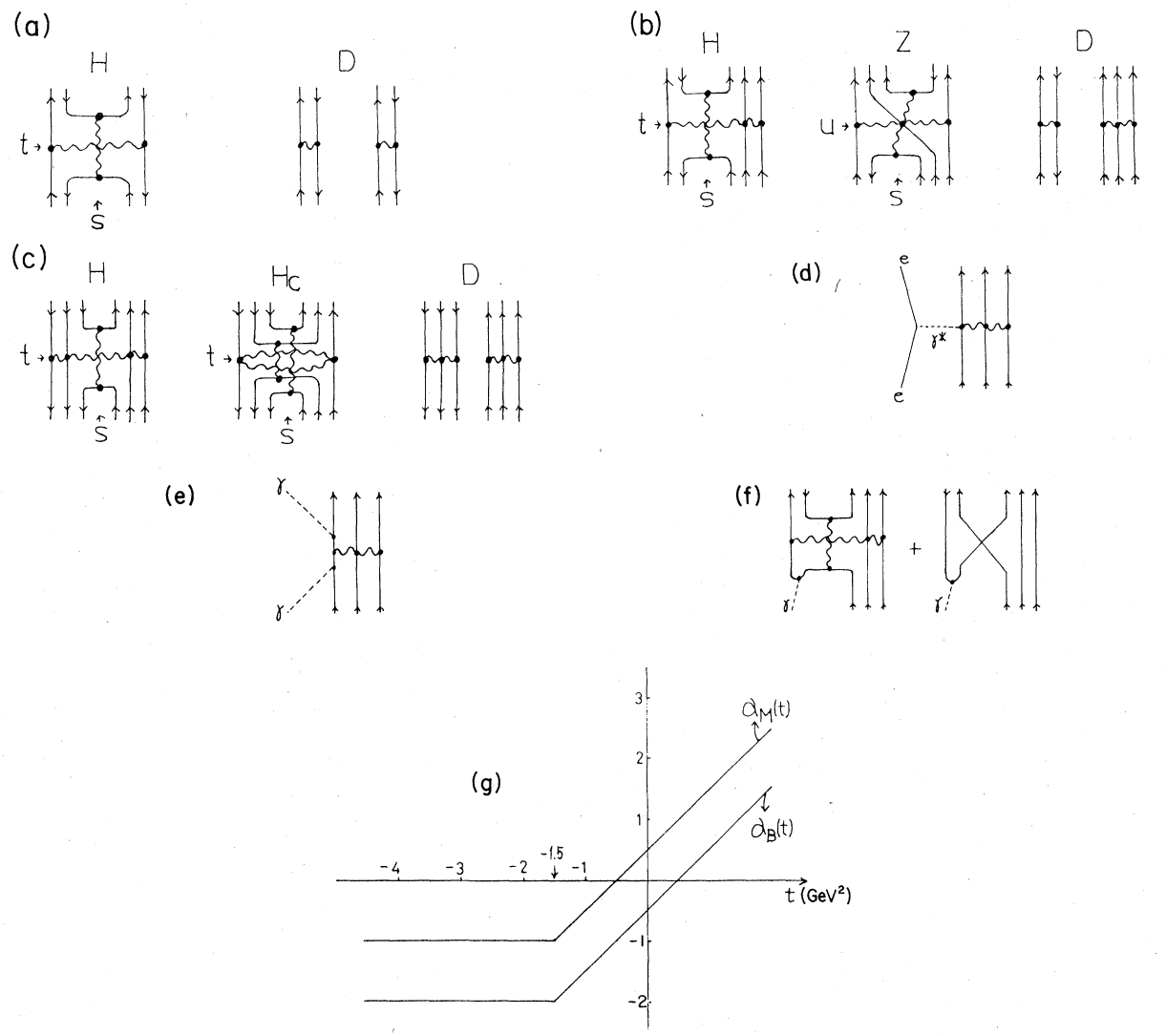

FIG. 2. Planar quark-line diagrams, (a) meson-meson scattering, (b) meson-baryon scattering, (c) antibaryon-baryon scattering, (d) $eB \to eB$, (e) $\gamma B \to \gamma B$, (f) $\gamma B \to MB$. (g) The effective trajectories for mesons and baryons.

The number of the hard strings is the most essential information to determine the energy and angular dependence of the amplitude, which is related to the configuration of quarks and strings. For s-t planar diagram, a hard string has t^{-1} dependence in the invariant amplitude in the s-channel bound state of quarks, and s^{-1} dependence in the t-channel bound state. For s-u planar diagram, a hard string has u^{-1} dependence in the s-channel bound state, and has s^{-1} dependence in the u-channel bound state.

On the basis of this hard-string effect the basic assumptions are as follows[14]:

(i) A hadron has the configuration of quarks combined by the strings even at large momentum transfer. In all the channels s, t, u this string configuration is conserved.

(ii) The number of strings in the bound state of quarks determines the power structure in s, t, and u of the invariant amplitude. For relevant diagrams the invariant amplitude satisfies s, t, u crossing relation and is given by the following law:

(a) For planar-type diagrams in Fig. 2, the number (n_i) of the hard strings in the bound state of quarks in the crossed channel of i channel determines the power energy dependence of i channel in a factorized form as

$$T = A\tilde{s}^{-n_s\gamma}\tilde{t}^{-n_t\gamma}\tilde{u}^{-n_u\gamma}, \quad \frac{d\sigma}{dt} = \frac{1}{16\pi}\frac{|T|^2}{s^2},$$

$\tilde{s} = (m^2 - s)/m^2$, $\tilde{t} = (m^2 - t)/m^2$ and $\tilde{u} = (m^2 - u)/m^2$, (2.1a)

where A, m, and γ are parameters, and γ equals unity at large angles. For example, n_s is the number of the hard strings in the t-channel bound state for the H-type diagram.

(b) For nonplanar-type diagrams, the amplitudes are obtained by s, t, u crossing relation.

(iii) The angular dependence of γ for q-$\bar{q}$ or q-q-q exchange corresponds to Regge-pole exchange forward and backward, and the γ parameter is connected to the analytic continuation of the linear rising Regge trajectory with the slope $\alpha = 1$ (see Fig. 2):

$-\gamma = \alpha_M(t) = t + 0.5$ for q-$\bar{q}$ exchange, (2.1b)

$-2\gamma = \alpha_B(t \text{ or } u) = t \text{ (or } u) - 0.5$ for q-q-q exchange,

where t is in GeV^2.

(1) In meson-baryon scattering, H-, X-(s-u obtained by crossing of H), and Z-type amplitudes in Fig. 2 are given:

(a) H-type amplitude (s-t dual):

$$T^H(s,t,u) \sim A_{MB}\tilde{s}^{-1}\tilde{t}^{-2} \text{ at large angles}$$
$$\sim A_{MB}\tilde{s}^{\alpha_M(t)}\tilde{t}^{-2}, \quad -t \lesssim 1.5 \text{ GeV}^2. \quad (2.2a)$$

(b) X-type amplitude (t-u dual) is given by s-u crossing of H:

$T^X(s,t,u) = T^H(s \leftrightarrow u)$ (the arrow expresses the crossing between two channels)

$$\sim A_{MB}\tilde{t}^{-2}\tilde{u}^{-1} \text{ at large angles},$$
$$\sim A_{MB}\tilde{t}^{-2}\tilde{u}^{\alpha_M(t)}, \quad -t \lesssim 1.5 \text{ GeV}^2,$$
$$\sim A_{MB}\tilde{t}^{\alpha_B(u)}\tilde{u}^{-1}, \quad -u \lesssim 1.5 \text{ GeV}^2. \quad (2.2b)$$

(c) Z-type amplitude (s-u dual):

$$T^Z(s,t,u) \sim A_{MB}\tilde{s}^{-2}\tilde{u}^{-2} \text{ at large angles},$$
$$\sim A_{MB}\tilde{s}^{\alpha_B(u)}\tilde{u}^{-2}, \quad -u \lesssim 1.5 \text{ GeV}^2. \quad (2.2c)$$

(2) In baryon-antibaryon $\rightarrow$ meson-meson scattering, the diagrams of H_t (obtained by s-t crossing of H), X_t (s-t crossing of X), and Z_t (s-t crossing of Z) types are considered for the amplitudes, which are obtained by s-t crossing of meson-baryon process.

(a) H_t-type amplitude:

$$T^{Ht}(s,t,u) = T^H(s \leftrightarrow t)$$
$$\sim A_{MB}\tilde{s}^{-2}\tilde{t}^{-1} \text{ at large angles},$$
$$\sim A_{MB}\tilde{s}^{\alpha_B(t)}\tilde{t}^{-1}, \quad -t \lesssim 1.5 \text{ GeV}^2. \quad (2.3a)$$

(b) X_t-type amplitude:

$$T^{Xt}(s,t,u) = T^X(s \leftrightarrow t)$$
$$\sim A_{MB}\tilde{s}^{-2}\tilde{u}^{-1} \text{ at large angles},$$
$$\sim A_{MB}\tilde{s}^{\alpha_B(u)}\tilde{u}^{-1}, \quad -u \lesssim 1.5 \text{ GeV}^2. \quad (2.3b)$$

(c) Z_t-type amplitude:

$$T^{Zt}(s,t,u) = T^Z(s \leftrightarrow t)$$
$$\sim A_{MB}\tilde{t}^{-2}\tilde{u}^{-2} \text{ at large angles},$$
$$\sim A_{MB}\tilde{t}^{-2}\tilde{u}^{\alpha_B(t)} \quad -t \lesssim 1.5 \text{ GeV}^2,$$
$$\sim A_{MB}\tilde{t}^{\alpha_B(u)}\tilde{u}^{-2}, \quad -u \lesssim 1.5 \text{ GeV}^2. \quad (2.3c)$$

(3) In baryon-(anti)baryon scattering,

(a) H-type amplitude as shown in Fig. 2:

$$T^H(s,t,u) \sim A_{BB}\tilde{s}^{-1}\tilde{t}^{-3} \text{ at large angles},$$
$$\sim A_{BB}\tilde{s}^{\alpha_M H}\tilde{t}^{-3}, \quad -t \lesssim 1.5 \text{ GeV}^2. \quad (2.4a)$$

(b) H_c-type amplitude, where double q-$\bar{q}$ states are exchanged in t channel and $q \supset \bar{q}$ state is in s channel:

$$T^{Hc}(s,t,u) \sim A_{BB}\tilde{s}^{-2}\tilde{t}^{-2} \text{ at all angles}, \quad (2.4b)$$

which has Regge-Regge cut contribution in the forward region, but its effect is neglected in our analysis.

(c) H_α-type amplitude, which is obtained by s-t crossing of H, and q-q-$\bar{q}$-$\bar{q}$ state is exchanged:

$$T^{Hd} = T^H(s \leftrightarrow t)$$
$$\sim A_{BB}\tilde{s}^{-3}\tilde{t}^{-1} \text{ at all angles}. \quad (2.4c)$$

(d) X-type amplitude (obtained by $s \leftrightarrow u$ crossing of H):

$$T^X(s,t,u) = T^H(s \leftrightarrow u)$$
$$\sim A_{BB}\tilde{t}^{-3}\tilde{u}^{-1} \text{ at all angles}$$
$$\sim A_{BB}\tilde{t}^{-3}\tilde{u}^{\alpha_M(t)}, \quad -t \lesssim 1.5 \text{ GeV}^2. \quad (2.4d)$$

(e) X_c-type amplitude ($s \leftrightarrow u$ crossing of H_c):

$$T^{Xc}(s,t,u) = T^{Hc}(s \leftrightarrow u)$$
$$\sim A_{BB}\tilde{t}^{-2}\tilde{u}^{-2} \text{ at all angles}. \quad (2.4e)$$

(f) X_d-type amplitude ($s \leftrightarrow u$ crossing of H_d):

$$T^{Xd}(s,t,u) = T^{Hd}(s \leftrightarrow u)$$
$$\sim A_{BB}\tilde{t}^{-1}\tilde{u}^{-3} \text{ at all angles}. \quad (2.4f)$$

(4) In photon-hadron scattering, we have the following. In $eB \rightarrow eB$ scattering, as shown in Fig. 2(d), two strings contribute to the baryon form factor, and in $eM \rightarrow eM$ scattering one string to

the meson form factor,

$$F_B(q^2)=f_B[m^2/(m^2-q^2)]^2 \text{ and } F_M(q^2)=f_M m^2/(m^2-q^2)\,. \tag{2.5a}$$

In $\gamma B \to \gamma B$ scattering, from Fig. 2(e), the invariant amplitude is

$$T_{\gamma B}(s,t,u)=A_{\gamma B}\tilde{t}^{-2}\,. \tag{2.5b}$$

In $\gamma B \to MB$ scattering, from Fig. 2(f), the amplitude is

$$\begin{aligned} T_{\gamma B\to MB}(s,t,u) &= (e_{q_1}T^H_{MB}+e_{q_2}T^X_{MB})/\sqrt{2} \\ &= A_{\gamma B\to MB}(e_{q_1}\tilde{s}^{-1}\tilde{t}^{-2}+e_{q_2}\tilde{t}^{-2}\tilde{u}^{-1})/\sqrt{2}\,e\,, \end{aligned} \tag{2.5c}$$

where e_{q_i} is quark charge. Here another possible counting law is as follows:

$$|T_{\gamma B\to MB}|^2=T_{\gamma B}(e_{q_1}T^H_{MB}+e_{q_2}T^X_{MB})/\sqrt{2}\,e\,. \tag{2.5d}$$

In Table I, the results of our counting law are listed.

III. ALL-ANGLE PHENOMENOLOGY

A. Baryon-(anti)baryon scattering

In baryon-antibaryon scattering, H-, H_c-, and H_d-type amplitudes contribute. The amplitude is written for $pp(n)$ scattering as

$$\begin{aligned} T_{\bar{p}p(n)}(s,t,u) &= A_{\bar{p}p(n)}\tilde{s}^{-\gamma}\tilde{t}^{-3\gamma}+A_{\bar{p}p(n)}\tilde{s}^{-2\gamma}\tilde{t}^{-2\gamma} \\ &\quad +A_{\bar{p}p(n)}\tilde{s}^{-3\gamma}\tilde{t}^{-\gamma}\,, \end{aligned} \tag{3.1a}$$

where $-\gamma=\alpha_M(t \text{ or } u)$ at $-t$ or $-u<1.5$ if n_s or $n_t=1$, and $\gamma=1$ in the other cases.

In baryon-baryon scattering, X-, X_c-, and X_d-type amplitudes contribute:

$$\begin{aligned} T_{pp(n)}(s,t,u) &= T_{\bar{p}p(n)}(s\leftrightarrow u) \\ &= A_{pp(n)}\tilde{t}^{-3\gamma}\tilde{u}^{-\gamma}+A_{pp(n)}\tilde{t}^{-2\gamma}\tilde{u}^{-2\gamma} \\ &\quad +A_{pp(n)}\tilde{t}^{-\gamma}\tilde{u}^{-3\gamma}\,, \end{aligned} \tag{3.1b}$$

where

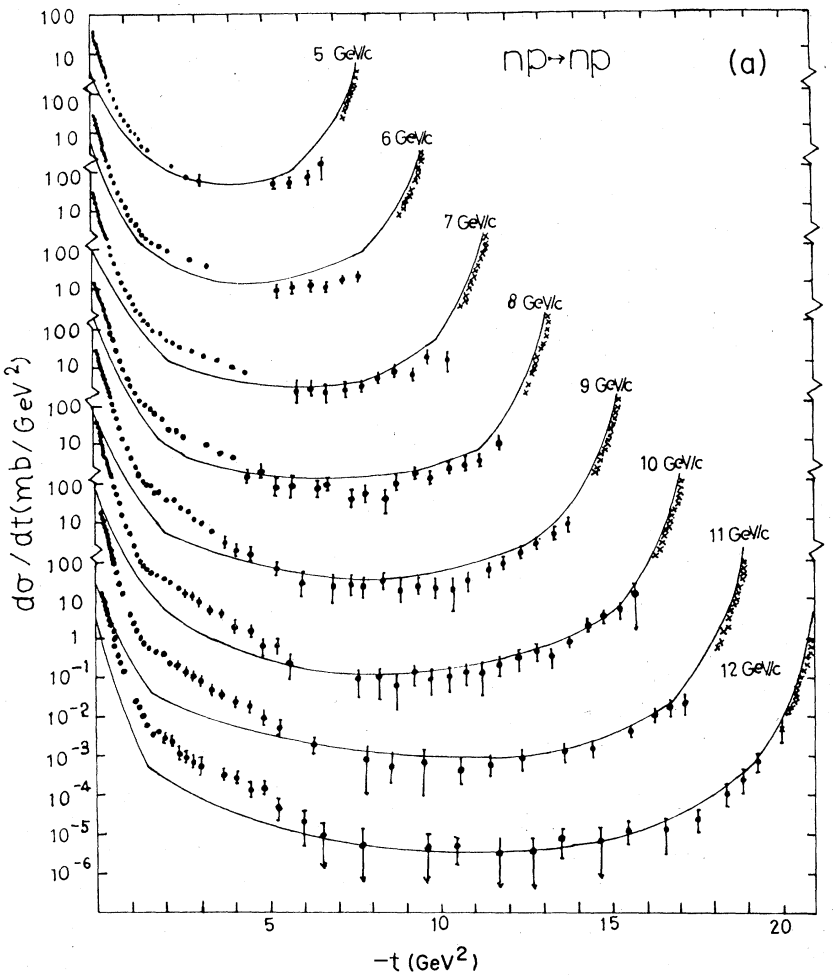

FIG. 3. The comparison of X-, X_c-, and X_d-type amplitudes with the experimental cross sections of $np \to np$ scattering and the comparison between $pp \to pp$ and $\bar{p}p \to \bar{p}p$ are shown (Refs. 3 and 6).

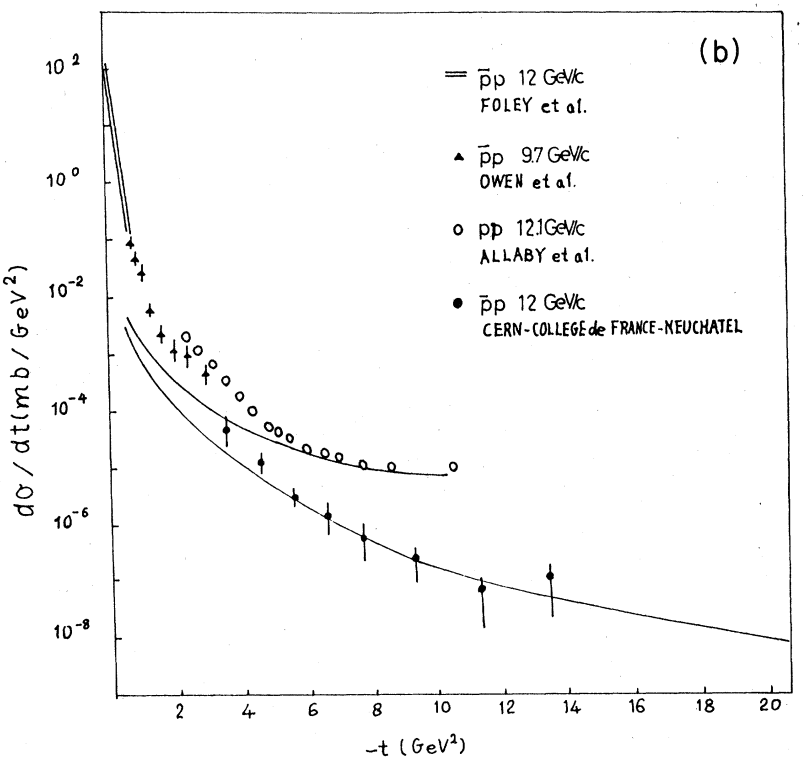

FIG. 3. (*Continued*)

$$A_{p\not{p}(n)} = A_{\bar{p}\not{p}(n)} .$$

In Fig. 3(a), our results are compared with the experimental ones in $pn \to pn$ at $P_L = 5$–12 GeV/c[3]. Since the diffractive-type amplitude contributes as much as the charge-exchange-type amplitude in experiments, our results have somewhat large deviation in the forward region. But, at large angles and in the backward region, the excellent consistency is obtained in both energy and angular dependence of the cross sections. The parameters are determined as follows:

$$A_{pn} = 75\sqrt{\text{mb}}\,\text{GeV}, \quad m^2 = 2.5\ \text{GeV}^2 . \tag{3.2}$$

In Fig. 3(b) the comparison between the cross sections of pp and $p\bar{p}$ elastic scatterings are shown at $P_L = 12$ GeV/c as

$$A_{pp} = 105\sqrt{\text{mb}}\,\text{GeV} \quad (= A_{\bar{p}p}) . \tag{3.3}$$

Our approach explains the large ratio of $d\sigma(pp)/dt/d\sigma(\bar{p}p)/dt$ well at large angles, because the difference of the phases between H_c and H_d suppresses $d\sigma(\bar{p}p)/dt$.[6,10,11]

In such processes as $\Sigma^-(\bar{\Sigma}^+)p \to \Sigma^-(\bar{\Sigma}^+)p$ and $n(\bar{\Delta}^+)p \to \Delta^-(\bar{n})\Delta^{++}$ the amplitude contains X- or H-type amplitude only except for the diffractive-type amplitude, then the ratios at $\theta_{\text{c.m.}} = 90°$ and $s \to \infty$ are

$$\frac{d\sigma(\Sigma^- p)/dt}{d\sigma(\bar{\Sigma}^+ p)/dt} = \frac{d\sigma(np)/dt}{d\sigma(\bar{\Delta}^+ p)/dt} = 4 . \tag{3.4}$$

B. Meson-baryon scattering

1. H-type process

In $K^- p \to \bar{K}^0 n$, H-type amplitude only contributes to the scattering. The qualitative feature of the cross section is reproduced very well at all angles in Fig. 4(a).[4,5] The reason for the deviation in the forward region may be considered for the flip amplitude to dominate, which is neglected in this paper.

2. X-type process

In $K^- p \to \pi^- \Sigma^+$, X- and Z-type amplitudes contribute. The X-type amplitude reproduces all-angle behavior qualitatively well at $P_L = 4.2$ GeV/c in Fig. 4(b).[5] The deviation at the dips is due to exchange-degenerate Regge-pole-like behavior of our model amplitudes. A Z-type amplitude explains the peak in the backward with the same parameters.

3. Z-type process

In $K^- p \to \pi^+ \Sigma^-$ and $\Sigma^-(1385)$, Z-type amplitude only contributes. Our results are compared with the experimental ones at $P_L = 4.2$ GeV/c.[5] Then the asymmetry of the cross section between the

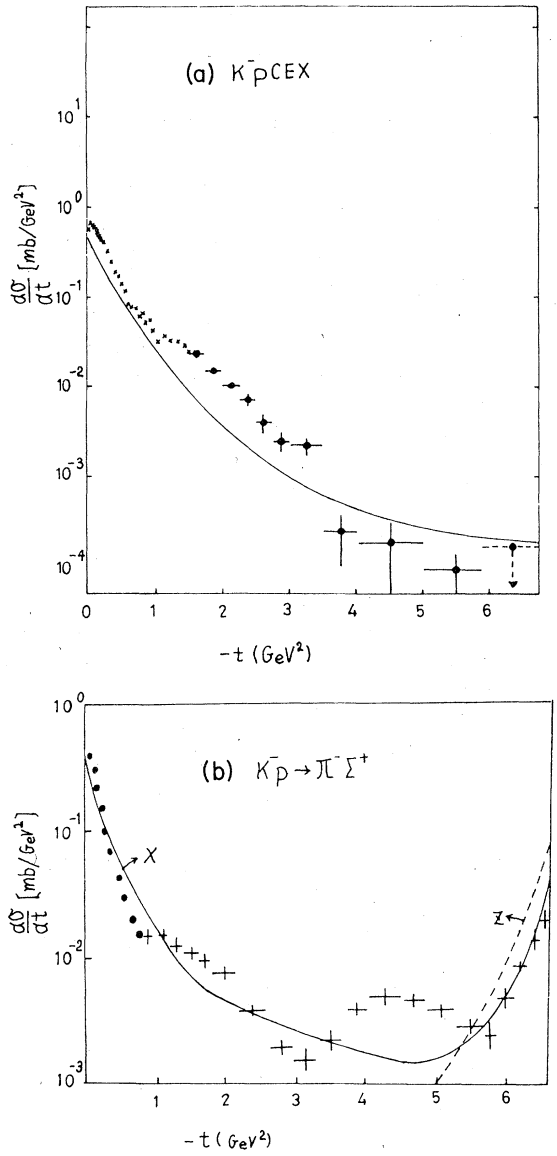

FIG. 4. The comparison of H- and X-type amplitudes with the experimental cross sections of $K^- p \to \bar{K}^0 n$ and $K^- p \to \pi^- \Sigma^+$ at $P_L = 4.2$ GeV/c (Refs. 4 and 5).

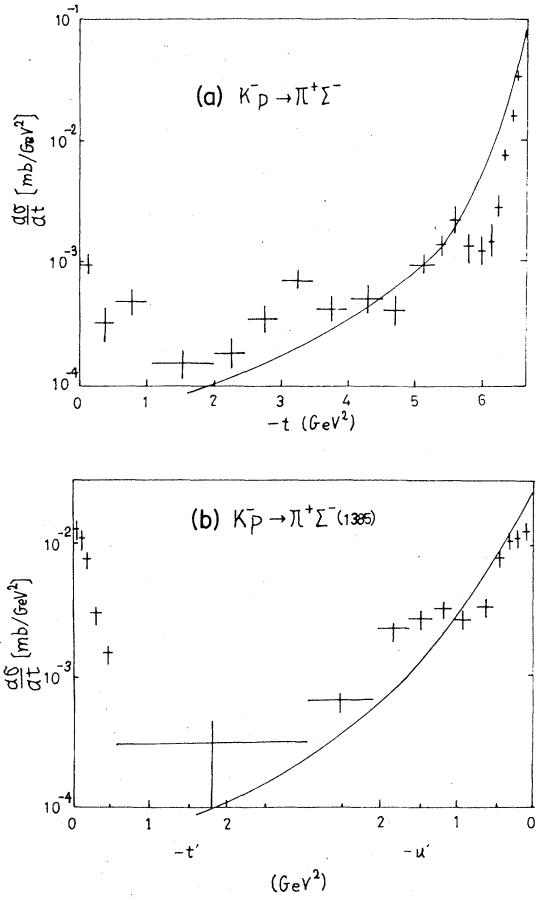

FIG. 5. The comparison of Z-type amplitude with the experimental cross sections of $K^- p \to \pi^+ \Sigma^-$ and $\pi^+ \Sigma^-$ (1385) at $P_L = 4.2$ GeV/c (Ref. 5).

forward and the backward is explained prominently by ours shown in Fig. 5. According to our model the energy dependence of the cross section at a fixed angle is the same as that of baryon-baryon scattering, that is, s^{-10} at $s \to \infty$.

In (1)–(3), we use the same parameters:

$$A_{MB} = 30\ \sqrt{\text{mb}}\,\text{GeV}, \quad m^2 = 2.5\ \text{GeV}^2. \tag{3.5}$$

Our approach is able to reproduce all-angle behavior qualitatively very well even for various nondiffractive processes.

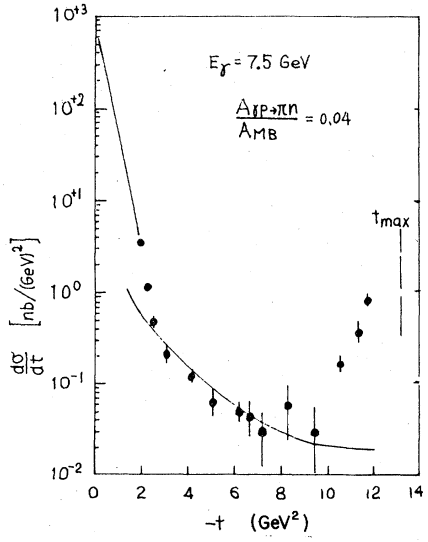

FIG. 6. The angular distribution of the cross section in $\gamma p \to \pi^+ n$ (Ref. 16).

C. Photon-baryon scattering

Our approach gives dipolelike behavior to the form factor of a baryon and monopolelike behavior to that of a meson in (2.5a). In Ref. 16 the experiment gives $d\sigma/dt \propto s^{-6}$ in $\gamma p \to \gamma p$ and s^{-8} in $\gamma p \to \pi^0 p$. These are consistent with the predictions of (2.5b) and (2.5c). The result of (2.5d) seems to be unfavorable. In Fig. 6 the angular dependence of our predicted cross section of (2.5c) is compared with the experimental cross section of $\gamma p \to \pi^+ n$. At large angles a favorable fit is obtained, but our parametrization is inadequate for unnatural-parity Regge-pole exchange in the forward direction, and the Z-type amplitude is needed for the explanation of the backward peak.

IV. DISCUSSION AND SUMMARY

We proposed a counting law on the basis of hadron structure with quarks and strings. Large-momentum-transfer phenomenology can show what the hadron structure is, and we can select the most useful model from various approaches. In particular, a counting law taking the junction by three strings into consideration in Ref. 10 gives the same phenomenology as ours to meson-meson and meson-baryon scattering except the Z-type process, but has difficulty in explaining the asymmetry of angular distribution of the cross section in $K^- p \to \pi^+ \Sigma^-$. On the other hand, the linearly rising Regge trajectory is shown to have the universal slope in both cases of mesons and baryons by the rotation of the extended hadron with linear-type structure. This structure seems to contribute to both small- and large-momentum-transfer region.

The results of our approach are summarized as follows:

(a) We arrive at the conclusion that the linear-type structure of a baryon is most powerful among the models proposed by analyzing the data of nondiffractive processes at all angles.

(b) Regge trajectories are connected universally to the γ parameter of fixed-angle scaling at $-t$ or $-u = 1.5$ GeV^2, where the breaking effect of exchange degeneracy and the contribution of Regge-Regge cut are not taken into account.

(c) At higher energy and large angles, the limiting scaling behavior should appear asymptotically.

(d) At $P_L \approx 3$–250 GeV/c our parametrization may reproduce the fixed-angle scaling behavior. At higher energy the breaking of q^{-2} dependence of a string may be observed in two-body scattering.

(e) Quantization of linear-type structure of hadrons should be investigated in the next step even at large momentum transfer. In quantum chromodynamics (QCD) we can obtain the same string configuration. But perturbative QCD gives the different effect from ours. Nonperturbative QCD may give the string configuration and its energy dependence. And perturbative QCD effect should be observed at higher energy at $P_T \gtrsim 8$ GeV.

ACKNOWLEDGMENT

The author would like to thank the members of the theoretical group in the institute of Hiroshima University for valuable discussion.

[1] M. Jacob and P. V. Landshoff, Phys. Rep. 48, 285 (1978).
[2] D. Sivers, R. Blankenbecler, and S. J. Brodsky, Phys. Rep. 23, 1 (1976).
[3] J. L. Stone *et al.*, Phys. Rev. Lett. 38, 1315 (1977).
[4] G. G. G. Massaro *et al.*, Phys. Lett. 66B, 385 (1977).
[5] F. Maszano *et al.*, Phys. Lett. 68B, 292 (1977); S. O. Holmgren *et al.*, Nucl. Phys. B119, 261 (1977).
[6] E. Nagy, in *Proceedings of the 19th International Conference on High Energy Physics, Tokyo, 1978*, edited by S. Homma, M. Kawaguchi, and H. Miyazawa (Phys. Soc. of Japan, Tokyo, 1979).
[7] M. Kawaguchi, Y. Sumi, and H. Yokomi, Phys. Rev. 168, 1556 (1968).
[8] V. A. Matveev, R. M. Muradyan, and A. V. Tavkhelidze, Lett. Nuovo Cimento 7, 719 (1973); S. J. Brodsky and G. R. Farrar, Phys. Rev. Lett. 31, 1153 (1973).
[9] Y. Igarashi, T. Matsuoka, and S. Sawada, Prog. Theor. Phys. 52, 618 (1974); K. Kinoshita and Y. Myozyo, Prog. Theor. Phys. 52, 1873 (1974).
[10] M. Imachi, S. Otsuki, and F. Toyoda, Prog. Theor. Phys. 55, 1211 (1976); M. Imachi, *ibid.* 56, 1832 (1976).
[11] R. Blankenbecler, S. Brodsky, and J. F. Gunion, Phys. Rev. D 18, 900 (1978).
[12] Y. Nambu, in *Symmetries and Quark Models*, edited by R. Chand (Gordon and Breach, New York, 1970); in Proceedings of the International Symposium on High Energy Physics, Tokyo, 1973 (unpublished); C. Rebbi, Phys. Rep. 12, 1 (1976), and references therein.
[13] M. Imachi, S. Otsuki, and F. Toyoda, Prog. Theor. Phys. 52, 341 (1974); 52, 346 (1974); 55, 551 (1976).
[14] F. Nakamura, Prog. Theor. Phys. 53, 1829 (1975); 56, 1657 (1976).
[15] R. D. Field and R. P. Feynman, Phys. Rev. D 10, 2590 (1977); R. P. Feynman, R. D. Field, and G. C. Fox, Phys. Rev. D 18, 900 (1978).
[16] M. A. Shupe *et al.*, Phys. Rev. Lett. 40, 271 (1978); R. L. Anderson *et al.*, Phys. Rev. D 14, 679 (1976).